Biophysical Journal Volume 65 October 1993 1620–1631

Trans-unsaturated Lipid Dynamics: Modulation of Dielaidoylphosphatidylcholine Acyl Chain Motion by Ethanol

Lauraine A. Dalton and Keith W. Miller

Department of Biological Chemistry and Molecular Pharmacology, Harvard Medical School, Boston, Massachusetts 02115, and Department of Anesthesia, Massachusetts General Hospital, Boston, Massachusetts 02114 USA

ABSTRACT Acyl chain dynamics of the *trans*-unsaturated lipid, dielaidoylphosphatidylcholine (DEPC), were studied by conventional and saturation transfer electron paramagnetic resonance spectroscopy of aqueous dispersions of DEPC spin labeled with lecithins having doxyl groups at positions 5, 10, and 14 on the *sn*-2 chain. The gel to liquid crystalline transition is concerted with simultaneous increases in rotational motion about the long axis of the acyl chain (libration) and in *gauche-trans* conformational interconversions (wobble). Relative to saturated lecithins at similar reduced temperatures the double bond (*a*) slowed libration by an order of magnitude in both phases, while wobble motions were several times slower, and (*b*) produced a pronounced stiffness of the acyl chain near the double bond. Ethanol (0–1.6 M), in addition to its well-known colligative effect on the phase transition, was found to decrease the bilayer order in a concentration-dependent manner. This effect was smaller in the gel than in the liquid crystalline phase, most pronounced next to the double bond, and weakest deep in the bilayer. Ethanol affected slow motions little in the gel phase but wobble and libration correlation times were markedly decreased in the liquid crystalline phase.

INTRODUCTION

Much is known about acyl chain segmental motion in saturated lecithins from a variety of spectroscopic techniques. In contrast, less information is available on lipids with unsaturated acyl chains, even though unsaturated lipids are more abundant in biological membranes. The importance of comparing the modulatory effect of *trans*-unsaturated lipids with saturated lipids in biological systems has recently been emphasized in epidemiological reports of adverse health effects associated with consumption of partially hydrogenated oils (Willett et al., 1993). In an individual lecithin molecule comprised of saturated acyl chains, each methylene segment possesses comparable degrees of freedom to adopt a variety of *gauche* and *trans* conformers (twists and kinks) with respect to its proximal and distal neighboring segments (Lange et al., 1986; Moser et al., 1989). Ensembles of saturated lecithins (as in bilayers) possess a flexibility gradient of allowable segment orientations.

Unsaturated lecithins are expected to differ from saturated homologs in two respects—two segments are fused together by a double bond, and the fixed geometry of the double bond creates a local offset of the chain axis. The ⟩C═C⟨ rigid unit has nearly twice the mass of a methylene (CH_2) segment, and its motion is retarded in comparison to the single-bonded methylene segments. These two effects tend to isolate the motions of the acyl chain sections between the glycerol backbone and the site of unsaturation from those between the double bond and the terminal methyl group. Consequently, in the lipid bilayer the temperature of the main gel to liquid crystalline phase transition of unsaturated lipids behaves as if the acyl chains were composed of semi-independent polymethylene sections separated by double bonds (Cevc, 1991). ^2H NMR studies have identified the positions of unsaturation as regions having atypical properties (Seelig and Waespe-Sarcevic, 1978; Seelig and Seelig, 1977; Baenziger et al., 1991).

The potency of ethanol and other low molecular weight general anesthetics correlates with their lipid solubility (Alifimoff et al., 1989). This relationship suggests that physical interaction of ethanol with the lipid bilayer underlies the mechanism of its pharmacological properties. The precise sites of ethanol interaction with the lipid bilayer are not elucidated at this time, but several lines of evidence (Napolitano and Herbette, 1984; Rowe et al., 1987; Diamond and Katz, 1974) suggest that ethanol associates with the polar region, and that its effects upon the hydrophobic interior of the bilayer may derive from surface perturbations propagating through the lipid array.

Many studies of ethanol-lipid interactions have focused on the gel to liquid crystalline phase transition of lipids with

Received for publication 7 May 1993 and in final form 2 July 1993.

Address reprint requests to Professor Keith W. Miller at Massachusetts General Hospital, Department of Anesthesia, White Building, Room 430, Boston, MA 02114. Tel.: 617-726-8985; Fax: 617-726-5845.

Abbreviations used: DEPC, 1,2-dielaidoyl-*sn*-glycero-3-phosphocholine; DMPC, 1,2-dimyristoyl-*sn*-glycero-3-phosphocholine; DPPC, 1,2-dipalmitoyl-*sn*-glycero-3-phosphocholine; NME, 100 mM NaCl, 10 mM MOPS, 0.1 mM EDTA, pH 7.4, buffer; *n*-PCSL, phosphatidylcholine containing the doxyl spin label substituent (4,4-dimethyl-3-oxazolinyloxy-) at the *n* position on the *sn*-2 acyl chain; EPR, electron paramagnetic resonance; ST-EPR, saturation transfer EPR; MOPS, 3-(*N*-morpholino)propanesulfonic acid; doxyl, the 4,4-dimethyl-3-oxazolinyloxy substituent; V_1, V_2, absorption EPR signals detected in phase at the first and second harmonics of the applied Zeeman modulation frequencies of 100 and 50 kHz, respectively; V_2', absorption ST-EPR phase quadrature (out of phase) signal detected at the second harmonic of the 50-kHz applied field modulation; S_n, EPR order parameter at segment *n* of the phosphatidylcholine acyl chain; ΔS, change in order parameter at segment *n* in the $P_{\beta'}$ ripple phase versus the L_α liquid crystalline phase; T_m, temperature of the main phase transition between the $P_{\beta'}$ and L_α phases.

0006-3495/93/10/1620/12 $2.00

saturated, rather than unsaturated, acyl chains (Rowe, 1983; Ohki et al., 1990; Sturtevant, 1982). The time-averaged location of ethanol in the polar interfacial region of the bilayer suggests that the mechanism of ethanol-induced gel phase melting may not be strictly analogous to that for thermally induced melting. Ethanol might either differentially perturb the acyl chains near the surface or interaction with the head group might be propagated along the chain.

Dielaidoylphosphatidylcholine (DEPC)[1] contains a midleaflet *trans* double bond at C_9-C_{10} and its main phase transition occurs in the range of 10.5° to 13.5°C (Wu and McConnell, 1975) which is convenient for study of bilayers dispersed in excess water. We have therefore chosen to compare the effect of temperature and ethanol upon the gel (or ripple) phase to liquid crystalline phase transition in DEPC. EPR and saturation transfer EPR methods provide access to doxyl segmental motion correlation times over several orders of magnitude (10^{-11} to 10^{-3} s). We have used these techniques to study the motion of doxylphosphatidylcholine guests having their reporter groups at the double bond and four methylene segments above and below it. Dimyristoylphosphatidylcholine, with a main phase transition at 22–23°C (Silvius, 1983) serves as the saturated lipid reference for segmental motion rates. A preliminary account of this work has been presented (Dalton and Miller, 1993).

EXPERIMENTAL PROCEDURES

Materials

DEPC (20 mg/ml in chloroform) and dimyristoylphosphatidylcholine (DMPC; 25 mg/ml in chloroform) were purchased from Avanti Polar Lipids (Alabaster, AL). The doxyl-substituted phosphatidylcholine spin labels were kindly provided by Dr. Anthony Watts (University of Oxford, UK). Ethanol (USP grade, 200 proof) was obtained from Aaper Alcohol and Chemical Co. (Shelbyville, KY). Buffer components (MOPS, NaCl, EDTA, and sodium azide) were obtained from Sigma Chemical Co. (St. Louis, MO) or from Fisher (Biotech Division, Fair Lawn, NJ). The EPR reference standard, potassium nitrosodisulfonate, was obtained from Alfa Inorganics (Beverly, MA).

Preparation of lipid vesicles

Multilamellar liposomes of DEPC containing 1% of either 5-, 10-, or 14-doxyl distearoylphosphatidylcholine (5-, 10-, or 14-PCSL) were prepared by the method of Pringle and Miller (1979). Aliquots of chloroform and EtOH stock solutions of host and guest, respectively, were evaporated to dryness under nitrogen, residual solvent was removed under vacuum (16 h), then buffer saturated with argon was added and the lipids were dispersed by vortexing. Five cycles of vortexing at 50°C alternated with cooling in ice were conducted to prepare liposomes (50 mg/ml) in buffer (100 mM NaCl, 10 mM MOPS, 0.1 mM EDTA, 0.1% sodium azide, pH 7.4; designated buffer NME). Liposomes of DMPC doped with 5-PCSL were prepared in a similar manner. Chilled samples were transferred to quartz capillaries 0.60 mm ID × 0.84 mm OD (Vitro Dynamics, Inc. Rockaway, NJ) in an argon atmosphere and the capillary was flame-sealed. The lipid dispersions were sedimented to the bottom of the capillary tube by brief (10 min, 4°C) centrifugation (Boggs et al., 1989) at 4000 rpm in a Sorvall SS-34 fixed-angle rotor fitted with an adapter. The column height of packed lipid vesicles was 10–12 mm, so that a cylindrical sample having uniform dielectric properties was present in the active region (Mailer et al., 1991) of the resonator, as recommended by Hemminga et al. (1984). Relative spin concentrations were determined by double integration of the V_1 EPR spectra or by triple integration of the low power second harmonic in phase V_2 spectra.

The ethanol concentration in each series of samples was adjusted by adding 0.25 volumes buffer (control) or NME containing 5-fold concentrated stock solutions of ethanol to separate aliquots of the liposomes in ReactiVials (Pierce Chemical Co., Rockford, IL) fitted with Teflon/silicone septum caps for maintenance of an argon atmosphere. The multilamellar liposome dispersions were permitted to equilibrate with ethanol-supplemented NME buffer for 24 h prior to transfer to capillaries. The final concentrations of ethanol in the *n*-PCSL/DEPC dispersions (40 mg of lipid per ml) ranged from 0 to 1.6 M.

Recording of V_1 and V_2 EPR and V_2' ST-EPR spectra

A Varian E-109 spectrometer equipped with a loop-gap resonator, Model XP-0201 from Medical Advances (Milwaukee, WI), was used. The microwave signal was amplified by an X-band field-effect transistor from Miteq (Hauppauge, NY) in the Varian E-102 bridge as described by Hubbell et al. (1987). The spectrometer was interfaced to a Dell 316SX computer with an analog to digital card from Real Time Devices (State College, PA) in conjunction with software and hardware from Scientific Software Services (Bloomington, IL). The magnetic field was externally ramped by a controller board from the Department of Engineering, University of Denver. Typical 100-Gauss sweeps of the magnetic field consisted of 2000 discrete field bins. Temperature was regulated using a modified Varian E-257 assembly. The loop-gap resonator was positioned inside a "Q-Band" size glass dewar (Wilmad, Buena, NJ) fabricated to accommodate the Varian heater-sensor element in the path of precooled air flow. Temperature was measured in the air flow around the resonator as well as within the loop-gap resonator ceramic body. Type T thermocouples (subminiature 40-gauge copper-constantan; Omega Engineering, Stamford, CT) positioned in the air-vent holes in the Macor ceramic body of the resonator and in the air flow path upstream from the resonator were connected to an Omega Engineering Model 412B digital temperature indicator.

Microwave field intensity was calibrated by measurement of broadening of the width of the narrow-line reference sample 0.09 mM potassium nitrosodisulfonate in 20 mM potassium carbonate, as described by Beth et al. (1983). The modulation field amplitude was calibrated at each frequency (100 kHz for V_1 and 50 kHz for V_2' and V_2) by overmodulated broadening of the reference sample (Poole, 1983). Conventional EPR V_1 spectra were recorded at incident microwave power of 0.05 mW, corresponding to an effective microwave field intensity ($B_{1\text{eff}}$) of 3.32 μT, with low modulation amplitude relative to linewidth (50 or 100 μT) and frequency of 100 kHz. The second-harmonic signals V_2 and V_2' were recorded at incident power levels of 0.05 and 3 mW corresponding to $B_{1\text{eff}}$ of 3.32 and 25.7 μT, respectively (Thomas et al., 1976; Hemminga et al., 1984). The low power V_2 and V_2' spectra served as references for auxiliary spin concentration calculations and self-null phase-sensitive detector settings, respectively. The magnetic field was modulated at 50 kHz with an amplitude of 500 μT for recording second harmonic signals detected at 100 kHz.

Analysis of spectra

Order parameters (S) were calculated from $A_{\max}$ and $A_{\min}$ (Fig. 1 *A*) with corrections as described by Griffith and Jost (1976). The ST-EPR V_2' amplitude ratio parameters were measured with a one-milliTesla interval between L″ and L and H″ and H (shown in Fig. 1 *D*) as specified by Squier and Thomas (1986). Correlation times were calculated from empirical polynomial equations (Horvath and Marsh, 1988) with L″/L, H″/H, and C′/C as arguments. "Wobble" correlation times calculated from the L″/L and H″/H parameters are attributed to reorientation of the nitroxide z axis away from alignment with the external magnetic field B_0 (Marsh, 1980), where the nitroxide z axis (p-π orbital) is parallel to the long axis of the acyl chain (Griffith and Jost, 1976). Rotation about the long axis, "libration," does not involve a change in the relative orientation of the nitroxide moiety with respect to the bilayer normal. A decrease in the L″/L and H″/H parameters

is associated with an increase in the rate of segmental wobble, i.e., *trans-gauche* isomerization motions involving a change in angle of the nitroxide with respect to the long chain axis. A decrease in the C′/C parameter provides a measure of increased rate of libration, i.e., rotations about the long axis (Marsh, 1980). Qualitative features of the central portion of the ST-EPR spectra of control and EtOH-containing samples are described in terms of the amplitudes at the local minima and maxima L*, C, C′, C″, and H* shown in Fig. 1 *D* (Fajer and Marsh, 1983).

RESULTS

EPR spectra of *n*-PCSL in DEPC codispersions

The changes in spectral shapes attending the gel to liquid crystalline phase transition of aqueous multilamellar DEPC dispersions are shown (Fig. 1) for *n*-PCSL guests in DEPC vesicles dispersed in NME buffer without ethanol. The V_1 EPR and V_2' ST-EPR spectra are shown in the left and right columns, respectively. Each row, top to bottom, contains gel phase (*solid line*) and liquid crystalline phase (*dashed line*) spectra for the 5-, 10- and 14-PCSL probes, respectively. In the top row, left panel, the splittings for analysis of EPR spectra, $2A_{max}$ and $2A_{min}$, are indicated by solid (4°C) and dashed lines (14°C), and, right panel, the amplitude parameters for analysis of ST-EPR spectra are annotated for the gel phase spectrum at 4°C. In the subsections below, the gel phase spectra for each depth will be discussed first and liquid crystalline phase spectra second.

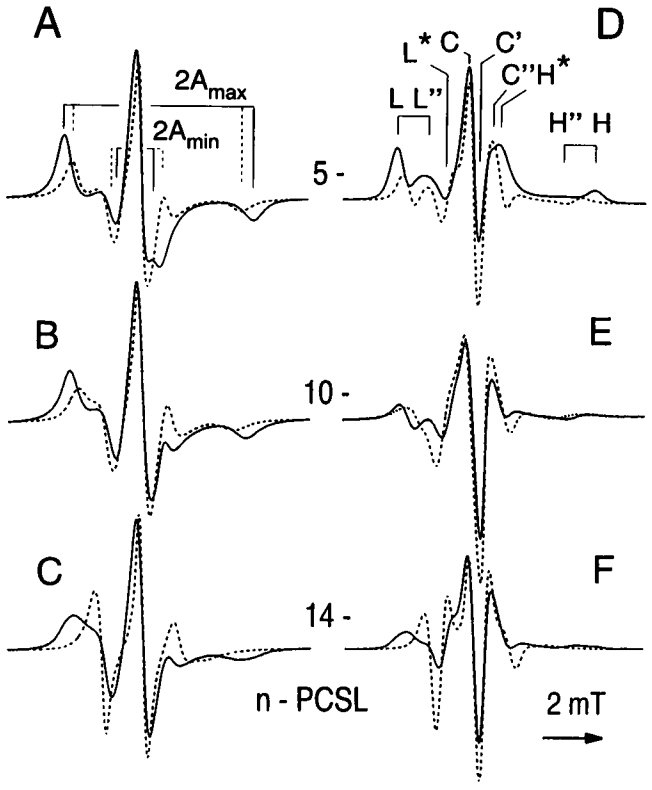

FIGURE 1 EPR (*left*; *A–C*) and ST-EPR (*right*; *D–F*) spectra of 5-, 10-, and 14-PCSL (*top* to *bottom*) guest in DEPC host multilamellar liposomes dispersed in NME buffer. Overlay plots of each sample at 4°C (*solid line*) and 14°C (*dashed line*) are shown. In each panel the pairwise overlays are normalized so that relative spin concentration (EPR, $\int\int V_1$; ST-EPR, $\int\int\int V_2$ at $B_1 = 3.32$ μT) and spectrometer gain are equivalent. Magnetic field scan width is 10 mT for all spectra.

Ripple-phase EPR spectra

In Fig. 1, ripple-phase spectra at 4°C are shown by solid lines. The overall spectral lineshape, i.e., a large A_{max} and small A_{min}, reflect hindered motion. The A_{max} splitting for 5-PCSL (Fig. 1 *A*), 6.36 mT, is in the range for the doxyl group in a strongly immobilized environment in terms of the time scale of motions detected by EPR.

EPR spectra of 10-PCSL (Fig. 1 *B*), with the doxyl substituent situated near the Δ_9 *trans* double bond of DEPC, have A_{max} less, and A_{min} greater, than their corresponding values in the spectra of 5-PCSL. This is consistent with a larger amplitude of segmental wobble motions which results in averaging of the A_z, A_y, and A_x elements of the doxyl hyperfine tensor.

At the 14-position near the center of the bilayer, the smaller A_{max} and larger A_{min} (Fig. 1 *C*) indicate that a greater angular distribution of orientations of the 14-doxyl acyl chain segment contribute to the ensemble-averaged EPR lineshape than for the 10- and 5-positions.

Ripple-phase ST-EPR spectra

Analysis of the ST-EPR spectrum of 5-PCSL in DEPC at 4°C (Fig. 1 *D*; *solid line*) yielded correlation times of 20, 35, and 2 μs derived from the L″/L, H″/H, and C′/C ratio parameters, respectively. Correlation times calculated from the H″/H ratio parameter were typically 1.5 times longer than those from the L″/L parameter, but the values were less precise due to the lower signal amplitude in the high field region. The 10-fold difference in effective correlation times for segmental wobble (L″/L and H″/H) in comparison to long axis rotation (C′/C) is typical for anisotropic motion in a lipid bilayer (Marsh, 1980; Delmelle et al., 1980).

The ST-EPR spectrum of 10-PCSL (Fig. 1 *E*) indicates that segmental wobble motion is significantly more rapid than for 5-PCSL under the same conditions. The L and H turning point positions have moved inward and their envelopes have changed shape, so that the distribution of spectral amplitudes above and below the baseline is more balanced than in Fig. 1 *D*. In other words, the first integral of the V_2' spectrum of 10-PCSL, normalized with respect to spin concentration, is much less than that for 5-PCSL at 4°C. This marked contrast in ST-EPR spectral shapes and integrated intensity of 5- and 10-PCSL provides motional rate information complementary to the orientational order information contained in the EPR spectra (which differ less noticeably). The H* region consists of a local minimum in 10-PCSL, whereas its amplitude in 5-PCSL is comparable to that of C″.

The 14-PCSL ST-EPR spectrum (Fig. 1 *F*) shows evidence of even more rapid motional averaging. The L and L″ regions have merged into a broad resonance with a high-field shoulder, and the C peak has acquired a low field shoulder which is better resolved in 14-PCSL than in

10-PCSL. The H position has moved inward relative to its position in 10-PCSL.

Liquid crystalline phase EPR and ST-EPR spectra

Spectra at 14°C, above the main gel to liquid crystalline phase transition (Wu and McConnell, 1975), are shown in Fig. 1 with dashed lines. For 5-PCSL (Fig. 1 *A*) melting decreases the EPR hyperfine splitting A_{max} due to motional averaging, and the correlation time for segmental wobble is within the range of sensitivity of EPR. The decrease in A_{max} is accompanied by an increase in A_{min}.

In the ST-EPR spectrum of 5-PCSL (Fig. 1 *D*, *dashed lines*) the increase in segmental wobble rate is recorded as inward shifts of the L and H positions. In addition, the depth of the C′ amplitude at 14°C in comparison to 4°C indicates that the rotation about the acyl chain long axis is more facile in the liquid crystalline phase. The central region of the ST-EPR spectrum of 5-PCSL at 14°C contains several features which are different from the gel-phase counterpart at 4°C. At 14°C, there is a shoulder between L* and C and the apparent width at half-height of C is less. The C″ peak has also narrowed at 14°C and the positive-amplitude peak at H* (at 4°C) has changed to a depression which is shifted outward toward H″. The overall shape of the V_2' ST-EPR spectrum at 14°C is similar to its V_2 (in phase) counterpart (not shown) in that there is a more nearly equal distribution of intensity above and below the baseline. Second, the normalized integral of the V_2' spectrum at 14°C is less than the integral of V_2' at 4°C.

The EPR spectrum of 10-PCSL at 14°C (Fig. 1 *B*) shows further motional averaging of the hyperfine splittings in comparison to 5-PCSL. The 14-PCSL probe (Fig. 1 *C*) has an EPR spectrum at 14°C indicative of considerable segmental wobble; the spectral shape is consistent with nearly isotropic motion of a weakly immobilized nitroxide.

The ST-EPR spectrum of 10-PCSL at 14°C (Fig. 1 *E*) shows evidence of merging of the L and L″ regions into a broad resonance with a slight high-field shoulder. The central region lineshape resembles a second derivative in that C and C″ are comparable in amplitude and they flank a deep depression at C′. The dip at H* is more negative than the corresponding region of the 5-PCSL ST-EPR spectrum. At 14°C, the 14-PCSL probe spectrum (Fig. 1 *F*) resembles the derivative of the EPR spectrum (1 *C*). There is substantial similarity in lineshape between the V_2 and V_2' spectra with the integrated intensity of V_2' being much lower than its in-phase counterpart V_2. For 10-PCSL, motion is so rapid that analysis of the EPR spectrum is more informative than examination of ST-EPR.

An approximate description of the spectral shape changes with lipid phase and bilayer depth is as follows: The 10-PCSL EPR and ST-EPR spectra at 4°C (Fig. 1, *B* and *E*, *solid lines*) resemble the 5-PCSL spectra at 14°C (Fig. 1, *A* and *D*, *dashed lines*). Likewise, at the 14-position near the center of the bilayer, the EPR spectrum (Fig. 1 *C*) at 4°C has an overall lineshape similar to that exhibited by 10-PCSL at 14°C, and this descriptive analogy is satisfactory for the ST-EPR spectra (Fig. 1 *F*) as well.

Ensemble-averaged order parameter versus depth

In Fig. 2, the results of analysis of V_1 EPR spectra in terms of the order parameter S (Hubbell and McConnell, 1971) are shown. As temperature increases from 0° to 10°C, the 5-PCSL senses a slight decrease in order in the gel phase, followed by a marked decrease (from 0.9 to 0.74) at 10–12°C in the main phase transition region, and concluded by a slight decrease in the liquid crystalline phase. The 10-PCSL order parameter undergoes a decrease comparable to 5-PCSL in the 0° to 10°C range, but in the phase transition region, 10–12°C, the decrease in S, from 0.7 to 0.63, is half that observed with 5-PCSL. In the liquid crystalline phase, S continues to decrease gradually with temperature.

At 0°C the order parameter drops markedly between the 5- and 10-positions but only by a small amount between the 10- and 14-positions. However, increasing temperature in the ripple phase is roughly twice as effective in causing disorder at the 14-position, so that at 10°C the order gradient is approximately linear. The decrease in order parameter in the phase transition region (from 0.54 to 0.27) is also more pronounced than for 5- and 10-PCSL.

ST-EPR measurement of motion in the ripple phase

Changes in motion in the ripple phase were examined using the ST-EPR method, wherein the spectral shape is sensitive

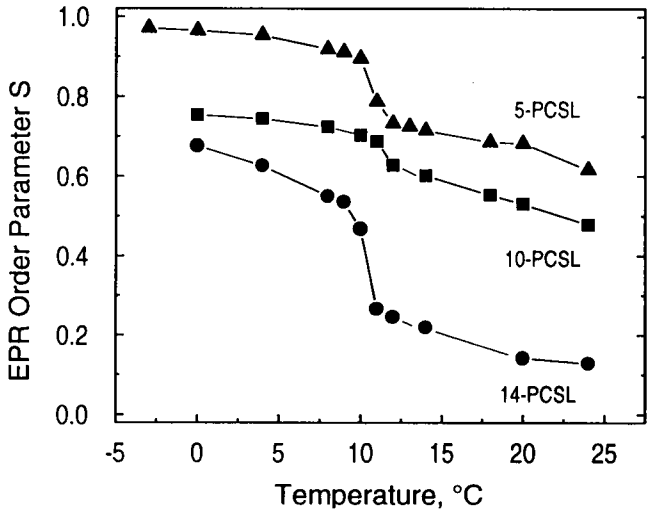

FIGURE 2 EPR order parameters, *S*, versus temperature for *n*-PCSL in DEPC liposomes at three different depths in the bilayer. The doxyl nitroxide substituent is located on the *sn*-2 acyl chain at positions 5 (*triangles*), 10 (*squares*), and 14 (*circles*). The relative temperature sensitivity of S_n is given by the slope, dS_n/dt. In the ripple phase, the slopes ($\times 10^{-3}$) for n = 5, 10, and 14 are −5.8 (±0.8), −5.0 (±1.0), and −16.0 (±1.1), respectively; in the liquid crystalline phase, the corresponding values are −9.4 (±2.1), −12.3 (±0.3), and −9.4 (±2.7).

to reorientation rates slower than the inverse of the hyperfine anisotropy (Hyde and Dalton, 1979). Fig. 3 illustrates the changes in spectral features for 5-PCSL codispersed with DEPC in NME buffer. The low and high field hyperfine resonance positions L and H for the nitroxide turning points are indicated for the spectrum at 0°C by the vertical dashed lines. The width of these resonances is comparable over the temperature range of 0° to 9°C, but the width increases by 10% at 10°C (1°C before melting). Throughout the ripple phase there is a gradual inward shift of resonance position with increasing temperature. The amplitudes at the intermediate positions, L″ and H″ (1.0 mT toward the center, relative to the L and H positions) decrease significantly and H″ approaches the baseline. The integral of V_2' decreases slightly with temperature in the ripple phase, then decreases sharply at the phase transition to approximately 15% of its average ripple phase value. As a control, these measurements were repeated with 5-PCSL in DMPC from 11° to 23.5°C; similar lineshape changes were observed (spectra not shown).

In the central region of the V_2' spectra, the depth of C′ increases with temperature. A more negative C′ amplitude (at constant C) is associated with decreasing correlation time for long axis rotation. Analysis of the extent of change with temperature of correlation times for segmental wobble (obtained from L″/L and H″/H) and libration (from C′/C) permits comparison of the selective onset of a particular motion prior to or correlated with the main phase transition (Marsh, 1980). Correlation times, given in Fig. 4, indicate that neither segmental wobble rates $(\tau(L''/L)^{-1})$ nor acyl chain long axis rotation rates $(\tau(C'/C)^{-1})$ change dramatically prior to the onset of the main phase transition.

The temperature profile of correlation times for wobble, $\tau(H''/H)$, and libration, $\tau(C'/C)$ for 5-PCSL codispersed with

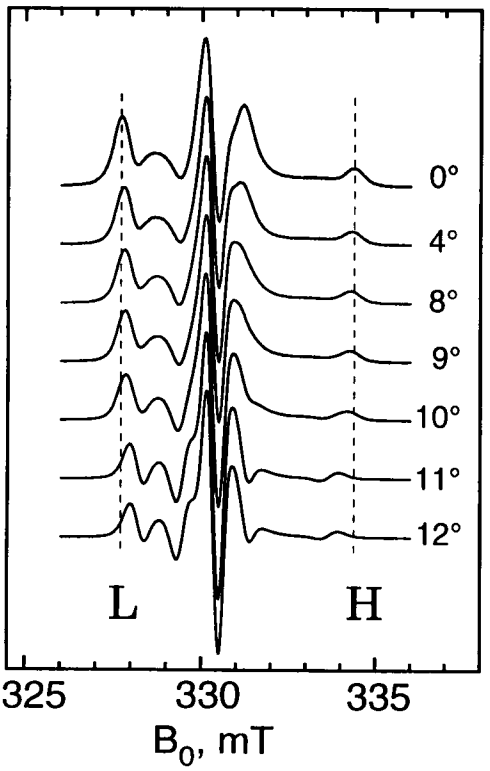

FIGURE 3 ST-EPR V_2' spectra for 5-PCSL in DEPC dispersions in NME buffer over the temperature range pertinent to the main phase transition from gel to liquid crystalline states. The spectral amplitude parameters L and H, which shifted inward as temperature was increased, were measured at low and high field maxima positions as shown by dashed lines on the 0°C spectrum. The L″ and H″ and C and C′ parameters were determined as in Fig. 1. Spectra are scaled so that the positive central excursions, C, are equivalent.

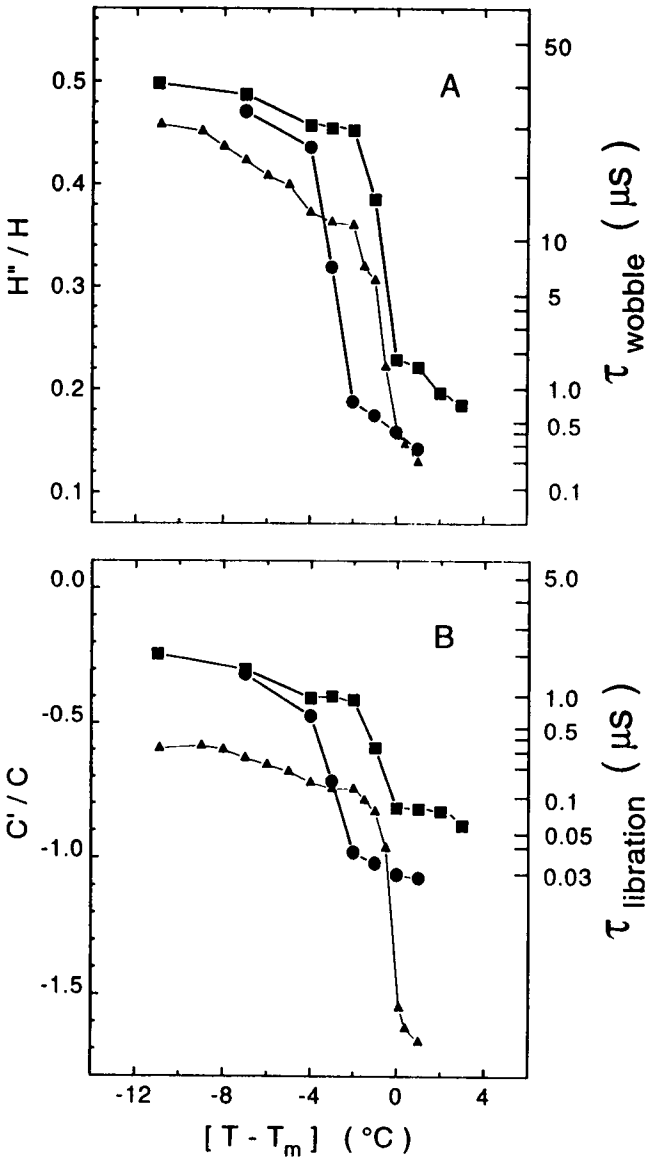

FIGURE 4 ST-EPR ratio parameters. (*A*) H″/H for 5-PCSL in DEPC in NME buffer (*square*), in buffer containing 1.2 M ethanol (*circle*), and for 5-PCSL in DMPC (*triangle*). (*B*) C′/C ratios. The abscissa scale is reduced temperature (observed temperature (T) – main phase transition temperature (T_m)). The values taken for T_m of DEPC and DMPC were 11° and 21°C, respectively. Although T_m for the EtOH-containing sample was depressed ~1°C lower than the control, the value of 11°C was used for calculation of $[T - T_m]$ of both samples for clarity of presentation. Effective correlation times, τ_{wobble} and $\tau_{libration}$, calculated from polynomial equation fits to H″/H and C′/C calibration curves (Horvath and Marsh, 1988), respectively, are indicated on the right ordinates of *A* and *B*. The minimum C′/C value for which the fit is valid is −1.0, corresponding to τ = 0.03 μs.

DEPC and with DMPC in NME buffer is shown in Fig. 4. Comparison of motion in different systems in Fig. 4 is made on a scale of "reduced temperatures," i.e., at similar temperature intervals below and above the main $P_{\beta'}$ to L_α phase transition temperature (T_m) for the respective lipids (Marsh and Watts, 1980). The prominent difference between the unsaturated DEPC and saturated DMPC acyl chain motion is the attenuation of long axis rotation (libration) in DEPC. Throughout the ripple phase, the correlation time for libration in DEPC, 2 μs, is 10 times longer than τ(C′/C) for DMPC. This attenuation of rotational motion in DEPC relative to DMPC is preserved even during melting. The decrease in the C′/C parameter for DEPC is about 60% of that observed for DMPC. The C′/C value for liquid crystalline DMPC (Fig. 4 *B*) is well below the lower limit, −1.0, of the calibration curve for correlation time (Horvath and Marsh, 1988), so the comparison of libration rates in the liquid crystalline state of these two lipids is necessarily qualitative. The wobble correlation times can be compared and the *trans* double bond increases the correlation time 5-fold (Fig. 4 *A*).

There are subtle changes in the central region of the ST-EPR spectra of 5-PCSL in DEPC in the ripple phase, notably the change in relative amplitudes of the positive region to the right of C′ (Fig. 3). There appear to be two components in this region, analogous to the positions C″ and H* (Fig. 1) defined for spin-labeled hemoglobin (Fajer and Marsh, 1983), but less resolved than for hemoglobin. Second, the apparent width of the positive excursion C peak increases with temperature, and upon transition to the liquid crystalline phase at 11°C, a distinct low-field shoulder separates from the C peak. The emergence of the low-field shoulder correlates with the appearance of a dip in the H* region. These spectral features are attributable to changes in anisotropic motion, but they are difficult to quantify in terms of correlation time because the motion at 11° and 12°C is fast on the ST-EPR time scale. Similar changes in the central portion of ST-EPR spectra of 5-PCSL in DMPC were observed prior to melting (data not shown).

The effect of ethanol on lipid order and dynamics

Inspection of Fig. 5, which shows the parallel relationship of EPR order parameter *S* versus temperature for ethanol-containing samples superimposed upon the corresponding plots for controls, reveals that the effect of ethanol upon the phase transition order parameter profile is limited. Ethanol's primary effect is to shift the abrupt decrease in *S* to lower temperature. The ethanol-induced decrease in T_m is of comparable magnitude for 5- and 10-PCSL in DEPC but this effect is propagated weakly to the interior of the bilayer monitored by 14-PCSL.

Analysis of the ST-EPR spectra of 5-PCSL/DEPC in NME buffer containing 0–1.6 M ethanol reveals that ethanol causes the decrease in correlation times for segmental wobble and libration to occur at lower temperatures (Fig. 4). In the ripple phase there is little effect on either motion but in the liquid crystalline phase large changes in both correlation times are

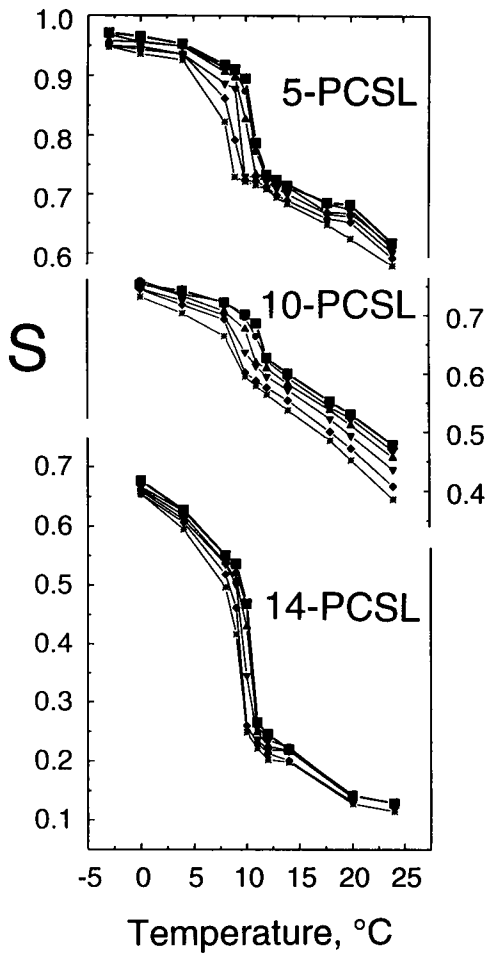

FIGURE 5 Plots of EPR order parameter, S, for three depths in the bilayer and six ethanol concentrations. The symbols correspond to ethanol concentration (in millimolar): ■, 0 (control); ●, 150; ▲, 400; ▼, 800; ◆, 1200; *, 1600.

observed with the librational correlation time being most affected. The librational correlation rate increases threefold as ethanol is varied from 0 to 1.6 M (Fig. 6).

For 5-PCSL, the motions associated with isothermal melting of the DEPC acyl chains induced by ethanol appear to be similar to melting caused by increased temperature (compare Fig. 7 and Fig. 3). At 4°C ethanol causes subtle changes in the ST-EPR lineshape (not shown), e.g., a change in relative amplitudes of C″ and H*. Changes in ST-EPR lineshape of 5-PCSL representative of ethanol-induced melting at 9°C are illustrated in Fig. 7; the lineshapes of samples with 0, 150, and 400 mM ethanol resemble the ripple phase low temperature spectra of Fig. 3, while the spectra of samples containing more than 800 mM ethanol resemble the high-temperature spectra of Fig. 3. Changes in lineshape in an isothermal set occur in a progressive fashion, e.g., at 7°C (not shown) only the sample with 1600 mM ethanol has a characteristic "melted" ST-EPR spectral shape and at 8°C (not shown) the 1200 and 1600 mM ethanol-containing samples possess this shape. At 9°C (Fig. 7) in the central region of the ST-EPR spectrum, elevated ethanol concentrations result

in the separation of a shoulder between L* and C, a deepening of the depression at C′, and the appearance of a depression between C′ and H″. The comparison of thermally induced and ethanol-induced melting is considered in more detail in the Discussion (Fig. 10).

DISCUSSION

Our aims in this investigation were to examine how segmental motions differ in unsaturated and saturated acyl chains and to identify the motions most affected by ethanol. A prominent feature of thermally induced melting of unsaturated lipids is that the acyl chain segments above and below the double bond behave separately, i.e., as if the lipid bilayer were composed of a sandwich of semi-independent polymethylene chains, each having an effective length demarcated by the glycerol backbone, double bond, and terminal methyl group. The ensemble of lipid molecules in a bilayer thus resembles a multilayered structure of thickness proportional to the effective chain lengths. This semiempirical model reliably predicts phase transition temperatures of a wide range of *cis*- and *trans*-unsaturated and saturated lipids (Cevc, 1991). Using Cevc's concepts as a starting point, we have performed a detailed investigation of motion and orientational order of spin label probes at three depths in the transverse plane of the bilayer, corresponding to the site of unsaturation and the midpoints of effective polymethylene chain lengths in the proximal and distal sections. The relative rates of two types of motion, rotation, or oscillation about the long axis (libration) and *gauche-trans* conformational interconversion (wobble), have been compared in saturated lipid bilayers of DMPC and DPPC (Marsh, 1980; Fajer et al., 1992). Corresponding data on unsaturated lipids were lacking at the time our DEPC studies were undertaken. One of the questions that interested us was whether the double bond, which provides a jog in the acyl chain, would retard librational motions. A subsidiary question is whether the double bond might also prevent the ethanol-induced interdigitation of acyl chains that is observed in saturated phosphatidylcholines (Rowe, 1983; Boggs et al., 1989; Nambi et al., 1988; Ohki et al., 1990).

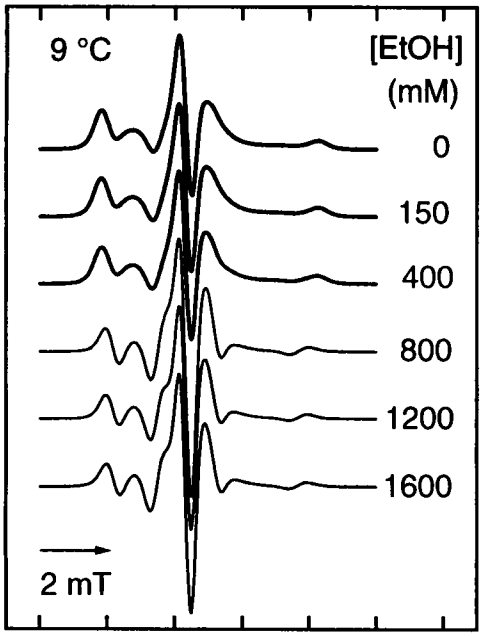

FIGURE 7 ST-EPR V_2' spectra of 5-PCSL/DEPC dispersions in NME buffer supplemented with ethanol. The concentration of ethanol (in millimolar) in the aqueous buffer is given to the right of each spectrum. At 9°C the control sample and samples containing 150 and 400 mM ethanol (*thick lines*) possessed lineshapes representative of ripple phase specimens while the samples containing 800, 1200, and 1600 mM ethanol (*thin lines*) had lineshapes diagnostic for the liquid crystalline phase, with progressive inward shifts of the L and H positions due to decrease of the wobble correlation time below the range of ST-EPR sensitivity. Sweep width is 10 mT; abscissa tick marks are at 2-mT intervals.

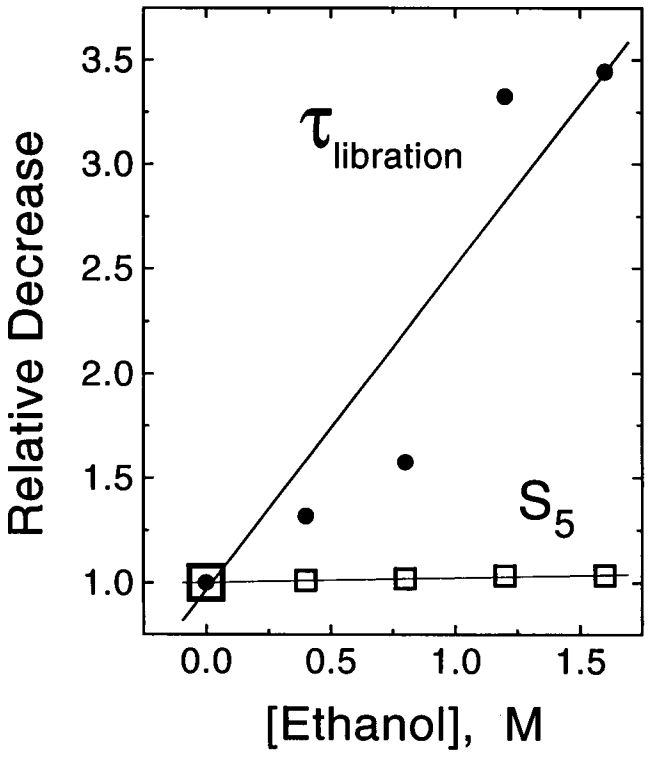

FIGURE 6 The relative decrease in correlation time for libration of 5-PCSL and order parameter S_5 as a function of ethanol concentration in the L_α phase at 12°C. The slope of the relative libration rate (*circles*) is 1.6 ± 0.3 M^{-1} ethanol. Similar behavior was observed for wobble correlation times (slope = 7.6 ± 2.7); data not shown. The order parameter (*squares*) changes minimally with increasing ethanol concentration; the relative decrease at 1.6 M ethanol is 1.03 (slope = 0.023 ± 0.003).

Slow motions in the proximal section of the acyl chains

Only in the proximal region of the acyl chains, that is, between the glycerol backbone and the double bond, were motions slow enough to apply ST-EPR techniques as well as conventional EPR. Hence, it is in this region that our conclusions are most complete. In the following section, orientational order in other regions of the bilayer will be considered.

To assess the effect of the double bond of DEPC upon motion, we compare our results on DEPC with those for DMPC (this work; Marsh, 1980; Fajer and Marsh, 1983; Moser et al., 1989; Subczynski et al., 1992; Fajer et al., 1992). It is appropriate to compare motion in these diverse systems at similar "reduced temperatures," i.e., at similar temperature intervals below and above the main $P_{\beta'}$ to L_α phase transition temperature (T_m) for the respective lipids (Marsh and Watts, 1980). T_m for DEPC, DMPC, and DPPC, are 12°, 23°, and 41°C, respectively (Silvius, 1983) and their lamellar $L_{\beta'}$ to ripple $P_{\beta'}$ pretransition temperatures are 11–12°C below T_m. Since our measurements on DEPC extend to 0°C as the lower limit, we have elected to compare characteristics of motion from $[T - T_m] = -10$°C to +3 for the three lipids. Thus our discussion will be limited to the $P_{\beta'}$ ripple phase and the L_α liquid crystalline phase.

Two classes of acyl chain motion, libration and segmental wobble, with correlation times given by τ(C′/C) and τ(L″/L) or τ(H″/H), respectively, have been measured from ST-EPR spectra of 5-PCSL in lecithin hosts in the gel phase. Libration simply consists of rotation or oscillation about the long axis of the acyl chain with minimal jostling of adjacent chains. In contrast, wobble motions, occurring within a cone of orientations relative to the normal to the bilayer, involve perturbation of adjacent chains. In the ripple phase of DEPC, the correlation times for wobble and libration differ by a factor of 20 (Fig. 4) with librational motions (τ(C′/C) ~ 1 μs) being faster than wobbling motions (τ(H″/H) or τ(L″/L) ~20 μs). The faster rate of libration relative to wobble is typical for anisotropic media such as gel-phase lipid acyl chains (Marsh, 1980; Marsh and Watts, 1980; Fajer et al., 1992).

As the reduced temperature increases in the ripple phase (from $[T - T_m] = -11°$ to −2°), this difference is maintained, but minor changes do occur in regions of the ST-EPR spectrum attributable to enhanced off-axial motions (Fajer and Marsh, 1983). For example, the amplitude parameters L*/L and H*/H decrease over the temperature range 0° to 9°C, as shown in the spectra in Fig. 3.

In the ripple phase of DEPC the librational and wobble correlation times decrease rapidly along the acyl chain; at 10-PCSL they are approximately 0.01 and ≪ 0.01 μs, respectively, and at 14-PCSL they are too rapid to measure. Composite correlation times for all types of reorientational motions were calculated from the inward shifts of hyperfine extrema of the conventional EPR spectra (McCalley et al., 1972) of *n*-PCSL in DEPC in the ripple phase. Defining the 5-PCSL time (τ = 0.04 μs at 0°C) as a reference value, τ for 10-PCSL and 14-PCSL are 4-fold and 6-fold shorter.

When the motions of 5-PCSL in the ripple phase of DEPC are compared to those in DMPC, two distinctive features are noted (Fig. 4). In the saturated lipids, the correlation time for libration is 8 to 10 times shorter than in DEPC at a given reduced temperature, whereas the correlation time for wobble is merely 1.5 to 2 times shorter. The librational correlation time of liquid crystalline DEPC at 12–14°C is comparable to that in ripple phase DMPC at the onset of the main phase transition. Even at comparable absolute temperatures, the ripple phase DMPC librational correlation time is only 3- to 4-fold slower than that in liquid crystalline DEPC. Also, the less well characterized off-axial motions evident in the L* and H* regions of the spectra (Fajer and Marsh, 1983) undergo parallel changes in both DEPC (Fig. 3) and DMPC (data not shown). Upon melting, the change in wobble rate is the same for DEPC and DMPC, indicating that the lateral interchain interactions have relaxed to about the same degree. On the other hand, the role of the double bond in restricting libration is still manifest in the liquid crystalline phase. In conclusion, the major consequence of introducing a *trans* double bond between the ninth and tenth carbons is restriction of librational motion with much less effect upon wobble motion.

Average orientational order in $P_{\beta'}$ and L_α phases

The order parameter at specific segments, S_n, provides information on the fractional distribution of *gauche* versus *trans* conformers as a function of depth in the bilayer. This order parameter depth gradient ("flexibility gradient") facilitates comparison of *n*-PCSL in DEPC with saturated lipid systems. In Fig. 8 DEPC and DPPC are compared close to their respective $P_{\beta'} \rightarrow L_\alpha$ phase transitions.

In the ripple phase at 4°C below T_m, both DEPC and DPPC exhibit an essentially linear decrease in order parameter with position, *n*, along the chain. Two characteristics of this decrease are noteworthy: First, the higher values of S_n for DEPC (Fig. 8, left panel) indicate a higher proportion of *trans*

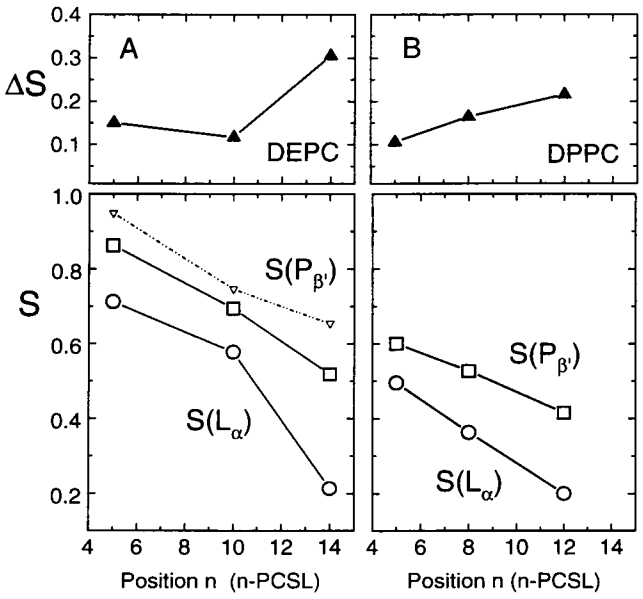

FIGURE 8 The order parameter, *S*, versus position *n* of the doxyl label in *n*-PCSL for DEPC (*A*, *left*) and DPPC (*B*, *right*) hosts. In the lower panels *S* for the ripple state ($P_{\beta'}$, *squares* and *inverted triangles*) and the liquid crystalline state (L_α, *circles*) is shown. The symbols, ▽, □, and ○ refer to data at reduced temperatures of −10, −4, and +1 with respect to T_m. T_m is 11°C for DEPC and 41°C for DPPC. In the upper panels ΔS refers to the difference in *S* between the ripple (−4°C) and liquid crystalline states (+1°), $\Delta S(P_{\beta'} \rightarrow L_\alpha)$. The DPPC data in *B* are from Hubbell and McConnell (1971).

conformers at all positions along the acyl chain, which is simply a consequence of the lower absolute temperature. The T_m for DEPC is 30°C below that for DPPC. Second, the population of *trans/gauche* conformers versus depth decreases comparably in both lipids.

In contrast, in the liquid crystalline phase at 1°C above T_m, the flexibility gradients for the unsaturated and saturated acyl chains differ markedly. In DEPC there is not a uniform decrease in *trans/gauche* conformer population with depth as in DPPC. The overall decrease in order parameter vs depth for both lipids is comparable between C-5 and C-14 (DEPC) or C-12 (DPPC), but the C-10 segment is more ordered than would be expected based on analogy with saturated lipids (Hubbell and McConnell, 1971; Subczynski et al., 1992; Seelig and Browning, 1978; Cevc and Marsh, 1987). The DEPC flexibility gradient is separated into two regions; *gauche/trans* conformational flexibility in the proximal region is attenuated and in the distal region it is amplified. The result of this behavior is that the change in order parameter upon melting, $\Delta S(P_{\beta'} \rightarrow L_\alpha)$, is much smaller at C-10 than at either C-5 or C-14, whereas in the saturated lipid it increases linearly with depth (Fig. 8, *upper panel*).

The unique characteristics of DEPC identified in this work are congruent with observations reported for unsaturated lipids studied by other methods. First, the enhanced temperature sensitivity of the 14-PCSL order parameter in the ripple phase (Fig. 2) indicates that the fraction of methylene segments in the *trans* conformation at C-14 (below the double bond) decreases more rapidly with temperature than at C-5 or C-10. The lower temperature sensitivity of S at C-5 and C-10 suggests relative confinement of the distribution of segment orientations, which is congruent with tethering of the proximal chain segment. The existence of a higher fraction of *gauche* conformers in DEPC than in saturated lipids has been postulated on the basis of neutron scattering measurements of bilayer thickness as a function of pressure (Winter et al., 1989). Another contribution to the elevated *gauche* conformer population could derive from additional cross section space made available by the slight vertical offset of *sn*-1 and *sn*-2 chains in the ripple phase (Seelig and Waespe-Sarcevic, 1978). Second, the retardation of libration of 5-PCSL in DEPC observed here (i.e., the smaller τ(wobble)/τ(libration) ratio for DEPC than DMPC in Fig. 4), is in accord with NMR observations on *cis*-unsaturated lipids (Baenziger et al., 1992). Third, the general stiffness of DEPC relative to DMPC has been documented by the diminished capability of termini of doxyl stearic acid guests to fold back and collide with labels in the proximal layer of the transverse plane (Yin et al., 1990).

The influence of the double bond is also evident on the slow motions detected by saturation transfer experiments. For example, in ripple phase DPPC (Fajer et al., 1992) the librational correlation time diminishes about an order of magnitude from the proximal end to the midpoint of the acyl chains—a change that is comparable to that in ripple phase DEPC. However, from the middle to the distal portion of the chain there is little further change in the librational correlation time in DPPC whereas in DEPC there is a further marked decrease in correlation time.

The effect of ethanol on acyl chain motion

Our main objective here was to study the action of ethanol on phospholipid dynamics. However, the information incidentally obtained on the depression of the main phase transition temperature by ethanol is broadly consistent with previous studies of saturated lipids which show that it takes place without changing the width (or cooperativity) of the transition (Rowe, 1983).

Overall, the action of ethanol on the bilayer dynamics was both phase- and depth-dependent. In the proximal acyl chain segments between the glycerol backbone and the double bond, reported by 5-PCSL, we were able to obtain the most information because both conventional and saturation transfer EPR could be employed. The detailed picture that emerges is that, in the ripple phase, ethanol has little effect on either wobble or librational motions (Fig. 4). In the liquid crystalline phase, both these characteristics become more sensitive to ethanol. For example, wobble and libration times are reduced threefold by the presence of 1.2 M ethanol. In contrast, the order parameter is much less sensitive to ethanol than are wobble and librational motions. For example, in 1.2 M ethanol the average decrease in order parameter S_n is 0.05 units, or 3% (Fig. 6).

The order parameter of the distal segments between the double bond and the terminal methyl group and the proximal segments nearer the glycerol backbone were almost equally sensitive to ethanol in both ripple and liquid crystalline phases (Fig. 9). Paradoxically, it was adjacent to the double bond, which in Cevc's model (1991) serves to isolate the two sections of the acyl chain, that the order parameter was most sensitive to the addition of ethanol in both P_β and L_α phases. Unfortunately, the rate of motion was sufficiently rapid that even in the ripple phase it was close to the limit of sensitivity of the saturation transfer technique and no further information could be obtained. An interesting possibility is that the time-averaged concentration of ethanol is higher near the double bond than in the rest of the acyl region due to the polarizability of the π electrons.

Comparison of temperature and ethanol-induced changes

It is instructive to compare the actions of ethanol to those of temperature. Changes in temperature were sensed by all sections of the bilayer, whereas those of ethanol may well depend on its unknown distribution throughout the bilayer. In the proximal segments next to the glycerol backbone, acyl chain motion is affected equally by ethanol and temperature, as is illustrated in Fig. 10. ST-EPR spectra of the control at 10° and 11°C are well matched by spectra of 5-PCSL/DEPC dispersions in ethanol-containing buffers at lower temperature. The lineshape parameters L″/L and H″/H are nearly identical for spectra in each column and the differences in

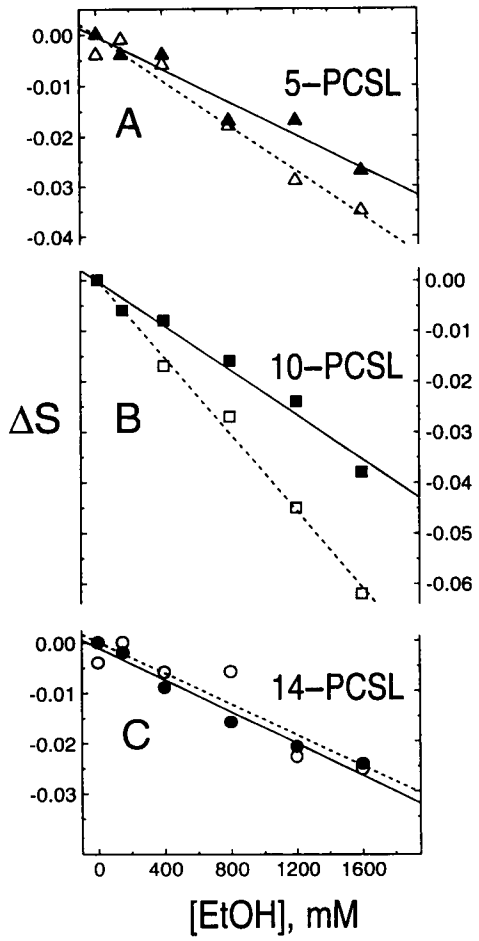

FIGURE 9 The change in order parameter as a function of ethanol concentration for the ripple phase at 4°C (*solid symbols*) and liquid crystalline phase at 14°C (*open symbols*) is shown for three depths in the bilayer. The labels, symbols, and slopes ($\times 10^{-5}$) are: 5-PCSL, ▲, −1.6, and △, −2.2; 10-PCSL, ■, −2.2 and □, −3.8; 14-PCSL, ●, −1.6 and ○, −1.6.

C′/C are small, indicating slightly faster libration in the presence of ethanol.

Analysis of librational correlation time data, such as those presented in Fig. 4 *B*, in terms of the temperature and ethanol concentration dependence yields insight into the relative magnitudes of change effected by these variables. The concentration of ethanol which effects a decrease in τ(C′/C) similar to that caused by a 1°C temperature increase is 150 mM in the ripple phase and 170 mM in the liquid crystalline phase. Thus, ethanol affects librational motion equivalently in both phases.

Similar analysis of the order parameter data presented in Fig. 5 yields the following "equivalent concentrations" of ethanol versus depth in the liquid crystalline phase: 400, 300, and 600 mM/°C for 5-, 10-, and 14-PCSL, respectively. Thus, ethanol enhances disorder in the proximal and midleaflet strata of the DEPC bilayer but is less potent in the distal region.

A priori there are two limiting causes which could explain why ethanol's ability relative to temperature to perturb acyl chain order declines with distance from the head group. First, ethanol might be uniformly distributed throughout the bilayer, but the intrinsic ability of each ethanol molecule to perturb adjacent segments of the acyl chain varies with depth. Second, ethanol's distribution across the bilayer could be nonuniform and the observed perturbations either reflect its local concentration or the ability of surface perturbations to propagate down the acyl chain. More detailed studies will be needed to establish the relative contributions of these factors. One readily available approach to these questions is to study interdigitation, because association of ethanol with lipid head groups is thought to be the cause of interdigitation in bilayers of saturated lipids (Rowe, 1983; Boggs et al., 1989). We used a protocol similar to that described by Boggs et al. (1989), i.e., slow cooling of samples and 24-h equilibration at temperatures well below the phase transition, with 14-PCSL/DEPC in NME buffer with and without 1.6 M ethanol. The V_1 and V_2' spectra of these two samples were identical. There was no evidence for a strongly immobilized component (with greater A_{max} splitting than the control) similar to that observed by Boggs et al. (1989). Our failure to detect interdigitation suggests that either the increased cross-sectional area associated with the double bond destabilizes this phase or that the offset in the acyl chain long axis restricts sliding motions, making the interdigitated phase kinetically more difficult to attain.

Physiological implications

From the viewpoint of the possible mechanisms of ethanol's physiological actions, two new findings may be significant. First, the importance of acyl chain unsaturation in modulating the action of ethanol is revealed. In the region of the double bond the disordering action of ethanol is enhanced, whereas deeper in the bilayer it is attenuated. If the same is true of more physiologically relevant lipids, investigation of the role of such differential action on the adaptation of lipid composition in the presence of ethanol ("membrane tolerance") would be germane.

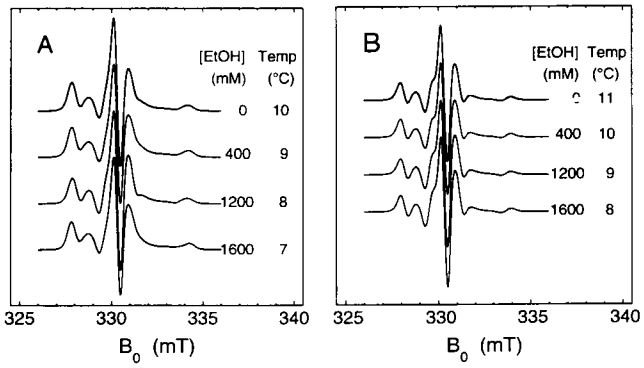

FIGURE 10 ST-EPR V_2' spectra of 5-PCSL in DEPC control samples (*top row*) in NME buffer at 10°C (*A*; *left*) and 11°C (*B*; *right*) with ethanol-containing samples at lower temperature having similar lineshapes underneath. Spectra are normalized so that the central peak amplitudes (*C*) with positive excursion above the baseline are equivalent.

Second, the rates of slow segmental wobble and librational motions are much more sensitive to the presence of ethanol than are measures of acyl chain conformational disorder such as the commonly reported order parameter. This may explain why in saturated lipids the $L_{\beta'} \rightarrow P_{\beta'}$ pretransition is much more sensitive to ethanol than the main ($P_{\beta'} \rightarrow L_{\alpha}$) transition (Janes et al., 1992), for in these lipids there is a marked increase in the rate of librational motions at the pretransition (Marsh, 1980). In order to quantify these concepts, we must take into account the marked temperature sensitivity of in vivo actions of ethanol. In mammals, threshold concentrations for anesthesia are in the range of 50 to 100 mM (Weiner et al., 1987). In tadpoles at 20°C, the anesthetic concentration is 200 mM, but at 10°C it is 340 mM (Alifimoff et al., 1989). An anesthetic concentration of 600 mM has been reported for *Daphnia magna* water fleas at 20°C (McKenzie et al., 1992) and at 10°C a twofold higher concentration is required. To correlate the influence of ethanol upon DEPC motion and orientational order with anesthetic effects, we note the following: for 5-PCSL in DEPC dispersions in 300 mM ethanol at 12°C, the librational correlation time decreases by a factor of 0.8 relative to the control in NME buffer, whereas the order parameter decreases less than 1% (Fig. 6). The ethanol concentration causing inebriation in poikilotherms at 12°C has yet to be reported. In mammals, the value is 10 to 20 mM ethanol, so that by analogy, an inebriating concentration of 50 to 100 mM in tadpoles at 12°C may be estimated, which corresponds to a 13–26% change in librational correlation time of 5-PCSL in DEPC.

We thank Dr. Anthony Watts of the University of Oxford for providing the spin-labeled lecithins and Drs. Derek Marsh and Piotr Fajer for helpful discussions.

Support from National Institute on Alcohol Abuse and Alcoholism (R01 AA07040 to K. W. Miller) is acknowledged. A Varian E-109 Century Series EPR spectrometer was kindly provided to the laboratory at Massachusetts General Hospital by Boston Biomedical Research Institute. This spectrometer was upgraded with assistance from Dr. Wayne Hubbell (Jules Stein Eye Research Institute at UCLA) and the National Biomedical ESR Center in Milwaukee, WI, whose help is gratefully acknowledged.

REFERENCES

Alifimoff, J. K., L. L. Firestone, and K. W. Miller. 1989. Anaesthetic potencies of primary alkanols: implications for the molecular dimensions of the anesthetic site. *Br. J. Pharmacol.* 96:9–16.

Baenziger, J. E., H. C. Jarrell, R. J. Hill, and I. C. P. Smith. 1991. Average structural and motional properties of a diunsaturated acyl chain in a lipid bilayer: effects of two cis-unsaturated double bonds. *Biochemistry.* 30: 894–903.

Baenziger, J. E., H. C. Jarrell, and I. C. P. Smith. 1992. Molecular motions and dynamics of a diunsaturated acyl chain in a lipid bilayer: implications for the role of polyunsaturation in biological membranes. *Biochemistry.* 31:3377–3385.

Beth, A. H., K. Balasubramanian, B. H. Robinson, L. R. Dalton, S. D. Venkataramu, and J. H. Park. 1983. Sensitivity of V_2' saturation transfer electron paramagnetic resonance signals to anisotropic rotational diffusion with [^{15}N]nitroxide spin-labels. Effects of noncoincident magnetic and diffusion tensor principal axes. *J. Phys. Chem.* 87:359–367.

Boggs, J. M., G. Rangaraj, and A. Watts. 1989. Behavior of spin labels in a variety of interdigitated lipid bilayers. *Biochim. Biophys. Acta.* 981: 243–253.

Cevc, G. 1991. How membrane chain-melting phase-transition temperature is affected by the lipid chain asymmetry and degree of unsaturation: an effective chain-length model. *Biochemistry.* 30:7186–7193.

Cevc, G., and D. Marsh. 1987. Phospholipid Bilayers: Physical Principles and Models. Wiley-Interscience. New York. 442 pp.

Dalton, L. A., and K. W. Miller. 1993. Phase behavior of dielaidoylphosphatidylcholine bilayers in the presence of ethanol studied by EPR. *Biophys. J.* 64:A74.

Delmelle, M., K. W. Butler, and I. C. P. Smith. 1980. Saturation transfer electron spin resonance spectroscopy as a probe of anisotropic motion in model membrane systems. *Biochemistry.* 19:698–704.

Diamond, J. M., and Y. Katz. 1974. Interpretation of nonelectrolyte partition coefficients between dimyristoyl lecithin and water. *J. Membrane Biol.* 17:121–154.

Fajer, P., and D. Marsh. 1983. Sensitivity of saturation transfer ESR spectra to anisotropic rotation. Application to membrane systems. *J. Magn. Reson.* 51:446–459.

Fajer, P., A. Watts, and D. Marsh. 1992. Saturation transfer, continuous wave saturation, and saturation recovery electron spin resonance studies of chain-spin labeled phosphatidylcholines in the low temperature phases of dipalmitoylphosphatidylcholine bilayers: effects of rotational dynamics and spin-spin interactions. *Biophys. J.* 61:879–891.

Griffith, O. H., and P. C. Jost. 1976. Lipid spin labels in biological membranes. *In* Spin Labeling: Theory and Applications. L. J. Berliner, editor. Academic Press. New York. 453–523.

Hemminga, M. A., P. A. de Jager, D. Marsh, and P. Fajer. 1984. Standard conditions for the measurement of saturation transfer ESR spectra. *J. Magn. Reson.* 59:160–163.

Horvath, L. I., and D. Marsh. 1988. Improved numerical evaluation of saturation transfer electron spin resonance spectra. *J. Magn. Reson.* 80:314–317.

Hubbell, W. L., and H. M. McConnell. 1971. Molecular motion in spin-labeled phospholipids and membranes. *J. Am. Chem. Soc.* 93:314–326.

Hubbell, W. L., W. Froncisz, and J. S. Hyde., J. S. 1987. Continuous and stopped flow EPR spectrometer based on a loop-gap resonator. *Rev. Sci. Instrum.* 58:1879–1886.

Hyde, J. S., and L. R. Dalton. 1979. Saturation-transfer spectroscopy. *In* Spin Labeling II: Theory and Applications. L. J. Berliner, editor. Academic Press. New York. 1–70.

Janes, N., J. W. Hsu, E. Rubin, and T. F. Taraschi. 1992. Nature of alcohol and anesthetic action on cooperative membrane equilibria. *Biochemistry.* 31:9467–9472.

Mailer, C., D. A. Haas, E. J. Hustedt, J. G. Gladden, and B. H. Robinson, B. H. 1991. Low-power electron paramagnetic resonance spin-echo spectroscopy. *J. Magn. Reson.* 91:475–496.

Marsh, D. 1980. Molecular motion in phospholipid bilayers in the gel phase: long axis rotation. *Biochemistry* 19:1632–1637.

Marsh, D., and A. Watts. 1980. Molecular motion in phospholipid bilayers in the gel phase: spin label saturation transfer ESR studies. *Biochem. Biophys. Res. Commun.* 94:130–137.

McKenzie, J. D., P. Calow, J. Clyde, A. Miles, R. Dickinson, W. R. Lieb, and N. P. Franks. 1992. Effects of temperature on the anaesthetic potency of halothane, enflurane and ethanol in *Daphnia magna* (cladocera: crustacea). *Comp. Biochem. Physiol.* 101C:15–19.

Moser, M., D. Marsh, P. Meier, K.-H. Wassmer, and G. Kothe. 1989. Chain configuration and flexibility gradient in phospholipid membranes: comparison between spin-label electron spin resonance and deuteron nuclear magnetic resonance, and identification of new conformations. *Biophys. J.* 55:111–123.

Nambi, P., E. S. Rowe, and T. J. McIntosh. 1988. Studies of the ethanol-induced interdigitated gel phase in phosphatidylcholines using the fluorophore 1,6-diphenyl-1,3,5-hexatriene. *Biochemistry.* 27:9175–9182.

Napolitano, C. A., and L. G. Herbette. 1984. An attempt to correlate the membrane localization of ethanol with functional perturbations in the calcium-pump ATPase of sarcoplasmic reticulum. *Biophys. J.* 45:317*a*. (Abstr.)

Ohki, K., K. Tamura, and I. Hatta. 1990. Ethanol induces interdigitated gel phase ($L_{\beta I}$) between lamellar gel phase ($L_{\beta'}$) and ripple phase ($P_{\beta'}$) in phosphatidylcholine membranes: a scanning density meter study. *Biochim. Biophys. Acta.* 1028:215–222.

Poole, C. P., Jr. 1983. Electron Spin Resonance: A Comprehensive Treatise

on Experimental Techniques. Wiley-Interscience. New York. 2nd ed. 780 pp.

Pringle, M. J., and K. W. Miller. 1979. Differential effects on phospholipid phase transitions produced by structurally related long-chain alcohols. *Biochemistry*. 48:3314–3320.

Rowe, E. S. 1983. Lipid chain length and temperature dependence of ethanol-phosphatidylcholine interactions. *Biochemistry*. 22:3299–3305.

Rowe, E. S., A. Fernandes, and R. G. Khalifah. 1987. Alcohol interactions with lipids: a carbon-13 nuclear magnetic resonance study using butanol labeled at C-1. *Biochim. Biophys. Acta*. 905:151–161.

Seelig, J., and J. L. Browning. 1978. General features of phospholipid conformation in membranes. *FEBS Lett.* 92:41–44.

Seelig, A., and J. Seelig. 1977. Effect of a single *cis* double bond on the structure of a phospholipid bilayer. *Biochemistry*. 16:45–50.

Seelig, J., and N. Waespe-Sarcevic. 1978. Molecular order in *cis* and *trans* unsaturated phospholipid bilayers. *Biochemistry*. 17:3310–3315.

Silvius, J. R.. 1983. Thermotropic phase transitions of pure lipids in model membranes and their modification by membrane proteins. *In* Lipid-Protein Interactions. P. C. Jost and O. H. Griffith, editors. Wiley. New York. Vol. 2. 239–281.

Squier, T. C., and D. D. Thomas. 1986. Methodology for increased precision in saturation transfer electron paramagnetic resonance studies of rotational dynamics. *Biophys. J.* 49:921–935.

Sturtevant, J. M. 1982. A scanning calorimetric study of small molecule-lipid bilayer mixtures. *Proc. Natl. Acad. Sci. USA*. 79:3963–3967.

Subczynski, W. K., E. Markowska, W. I. Gruszecki, and J. Sielewiesiuk. 1992. Effects of polar carotenoids on dimyristoylphosphatidylcholine membranes: a spin-label study. *Biochim. Biophys. Acta*. 1105:97–108.

Thomas, D. D., L. R. Dalton, and J. S. Hyde. 1976. Rotational diffusion studied by passage saturation transfer electron paramagnetic resonance. *J. Chem. Phys.* 65:3006–3024.

Weiner, N., J. K. Disbrow, T. A. French, and J. M. Masserano. 1987. The influence of catecholamine systems and thyroid function on the action of ethanol in long-sleep (LS) and short-sleep (SS) mice. *Ann. N. Y. Acad. Sci.* 492:375–383.

Willett, W. C., M. J. Stampfer, J. E. Manson, G. A. Colditz, F. E. Speizer, B. A. Rosner, L. A. Sampson, and C. H. Hennekens. 1993. Intake of *trans* fatty acids and risk of coronary heart disease among women. *Lancet*. 341:581–586.

Winter, R., C.-L. Xie, J. Jonas, P. Thiyagarajan, and P. T. T. Wong. 1989. High-pressure small-angle neutron scattering (SANS) study of 1,2-dielaidoyl-*an*-glycero-3-phosphocholine bilayers. *Biochim. Biophys. Acta*. 982:85–88.

Wu, S. H., and H. M. McConnell. 1975. Phase separations in phospholipid membranes. *Biochemistry*. 14:847–854.

Yin, J.-J., J. B. Feix, and J. S. Hyde. 1990. Mapping of collision frequencies for stearic acid spin labels by saturation-recovery electron paramagnetic resonance. *Biophys. J.* 58:713–720.